

UCSF

UC San Francisco Previously Published Works

Title

Enzymatic deglycosylation converts pathogenic neuromyelitis optica anti-aquaporin-4 immunoglobulin G into therapeutic antibody

Permalink

<https://escholarship.org/uc/item/6r0601jh>

Journal

Annals of Neurology, 73(1)

ISSN

0364-5134

Authors

Tradtrantip, Lukmanee
Ratelade, Julien
Zhang, Hua
[et al.](#)

Publication Date

2013

DOI

10.1002/ana.23741

Peer reviewed



Published in final edited form as:

Ann Neurol. 2013 January ; 73(1): 77–85. doi:10.1002/ana.23741.

ENZYMATIC DEGLYCOSYLATION CONVERTS PATHOGENIC NEUROMYELITIS OPTICA ANTI-AQUAPORIN-4 IgG INTO THERAPEUTIC ANTIBODY

Lukmanee Tradtrantip, Ph.D., Julien Ratelade, Ph.D., Hua Zhang, Ph.D., and A.S. Verkman, M.D., Ph.D.

Departments of Medicine and Physiology, University of California, San Francisco CA, 94143-0521, U.S.A

Abstract

Objective—Neuromyelitis optica (NMO) is caused by binding of pathogenic autoantibodies (NMO-IgG) to aquaporin-4 (AQP4) on astrocytes, which initiates complement-dependent cytotoxicity (CDC) and inflammation. We recently introduced mutated antibody (aquaporumab) and small-molecule blocker strategies for therapy of NMO, based on prevention of NMO-IgG binding to AQP4. Here, we investigated an alternative strategy involving neutralization of NMO-IgG effector function by selective IgG heavy-chain deglycosylation with bacteria-derived endoglycosidase S (EndoS).

Methods—Cytotoxicity and NMO pathology were measured in cell and spinal cord slice cultures, and in mice exposed to control or EndoS-treated NMO-IgG.

Results—EndoS treatment of NMO patient serum reduced by >95 % CDC and antibody-dependent cell-mediated cytotoxicity (ADCC), without impairment of NMO-IgG binding to AQP4. Cytotoxicity was also prevented by addition of EndoS after NMO-IgG binding to AQP4. The EndoS-treated, non-pathogenic NMO-IgG competitively displaced pathogenic NMO-IgG bound to AQP4, and prevented NMO pathology in spinal cord slice culture and mouse models of NMO.

Interpretation—EndoS deglycosylation converts pathogenic NMO-IgG autoantibodies into therapeutic blocking antibodies. EndoS treatment of blood may be beneficial in NMO, which may be accomplished, for example, by therapeutic apheresis using surface-immobilized EndoS.

Key terms

NMO; Devic's disease; AQP4; neuroinflammation; blocking antibody

INTRODUCTION

Neuromyelitis optica (NMO) is an inflammatory demyelinating disease primarily affecting spinal cord and optic nerve, producing paralysis and blindness.^{1,2} Most NMO patients are seropositive for immunoglobulin G (IgG) autoantibodies (NMO-IgG)^{3,4} against aquaporin-4 (AQP4), a plasma membrane water transporting protein expressed on astrocytes throughout the central nervous system.^{5,6} It is believed that NMO-IgG binding to AQP4

Manuscript correspondence to: Alan S. Verkman, M.D., Ph.D., 1246 Health Sciences East Tower, University of California, San Francisco CA 94143-0521, USA; Phone 415-476-8530; Fax 415-665-3847; Alan.Verkman@ucsf.edu; <http://www.ucsf.edu/verklab>.

Potential Conflicts of Interest. Drs. Verkman and Tradtrantip are named co-inventors on a patent application filed on EndoS therapy of NMO. The intellectual property is owned by the University of California.

initiates complement- and cell-mediated astrocyte cytotoxicity, resulting in inflammation, disruption of the blood-brain barrier, and secondary damage to oligodendrocytes and neurons.⁷ Current NMO therapies, which have limited efficacy and potential long-term side effects, include immunosuppression, plasma exchange, and B-cell-depleting monoclonal antibodies.^{8,9} An open label clinical trial of an anti-complement antibody therapy (eculizumab) is in progress.

We recently introduced a new therapeutic strategy for NMO, focused on prevention of the initiating pathogenic event of NMO-IgG binding to AQP4. In one approach, a tight-binding recombinant monoclonal antibody, derived from clonally expanded plasma blasts in NMO cerebrospinal fluid, was mutated to inhibit its effector functions for complement-dependent cytotoxicity (CDC) and antibody-dependent cell-mediated cytotoxicity (ADCC).¹⁰ The mutated, non-pathogenic antibody ('aquaporinab') competes with pathogenic NMO-IgG for AQP4 binding, preventing CDC, ADCC, and the development of NMO lesions in mouse models. In a second approach, high-throughput screening identified small-molecule blockers that bind to AQP4 and sterically prevent NMO-IgG binding to the extracellular surface of AQP4.¹¹

Here, we investigated the possibility of selective enzymatic deglycosylation of patient NMO-IgG to neutralize its effector function without affecting its binding to AQP4, thus converting pathogenic NMO-IgG into therapeutic blocking antibodies. Glycosylation of a conserved asparagine (Asn-297) on the CH2 domain of IgG heavy chains is essential for antibody effector functions.¹² Modification of the Fc glycan alters IgG conformation and reduces the Fc affinity for binding of complement protein C1q and effector cell receptor FcR.¹³ Complete removal of the Fc glycan abolishes CDC and ADCC. Endoglycosidase S (EndoS) is a 108 kdalton enzyme encoded by gene *ndoS* of *Streptococcus pyogenes* that selectively digests asparagine-linked glycans on the heavy chain of all IgG subclasses, without action on other immunoglobulin classes or other glycoproteins.¹⁴ EndoS has been used to neutralize pathogenic IgG in experimental animal models of autoimmunity, including collagen-induced arthritis,¹⁵ immune thrombocytopenic purpura,¹⁶ lupus erythematosus,¹⁶ and anti-neutrophil cytoplasmic autoantibody (ANCA)-mediated glomerulonephritis.¹⁷ Although EndoS has not been used in humans, a different glycosidase is in phase II clinical trials to neutralize blood group antigens to generate, *ex vivo*, universal blood for donation.^{18,19} We demonstrate here that EndoS treatment of NMO patient serum neutralizes its pathogenicity without affecting AQP4 binding, and demonstrate its utility in preventing NMO pathology in cell culture, organ culture and mouse models.

METHODS

Cell culture and antibodies

Chinese hamster ovary (CHO) cells stably expressing human M23-AQP4 were generated as described²⁰ and cultured at 37 °C in 5% CO₂/95% air in F-12 Ham's Nutrient mix medium supplemented with 10% fetal bovine serum, 200 µg/mL geneticin (selection marker), 100 units/mL penicillin and 100 µg/mL streptomycin. U87MG cells (human astrocytoma-derived) expressing human M23-AQP4 were generated and cultured as described.²⁰ Recombinant monoclonal NMO antibody rAb-53 (referred to as NMO-IgG) was generated from a clonally expanded plasma blast population from cerebrospinal fluid (CSF) of an NMO patient, as described and previously characterized.^{20,21} NMO serum was obtained from NMO-IgG seropositive individuals who met the revised diagnostic criteria for clinical disease.²² Non-NMO (seronegative) human serum was used as control. For some studies IgG was purified from NMO or control serum using a Melon Gel IgG Purification Kit (Thermo Fisher Scientific, Rockford, IL) and concentrated using Amicon Ultra Centrifugal Filter Units (Millipore, Billerica, MA).

EndoS treatment

EndoS was purchased from Bulldog Bio Inc. (Rochester, NY). NMO-IgG or NMO serum (or control IgG/serum) was incubated with EndoS (1 unit per 1–10 μg IgG) for up to 1 h at 37 °C. EndoS was not removed after treatment. In some experiments NMO serum was treated with EndoS using a microspin column containing EndoS covalently coupled to agarose beads. Treated antibody is referred to as NMO-IgG^{GL-}. Treated NMO serum is referred to as NMO serum^{GL-}. EndoS treatment efficiency was assessed by 10% sodium dodecyl sulfate polyacrylamide gel electrophoresis (SDS-PAGE) followed by staining with Coomassie Blue or *Lens culinaris* agglutinin (LCA)-lectin blot analysis, as described.¹⁶

NMO-IgG binding

Cells were grown on glass coverslips for 24 h. After blocking with 1% BSA in PBS, cells were incubated with NMO-IgG or NMO serum (control or EndoS-treated) for 1 h at room temperature. Cells were washed with PBS and incubated with Alexa-Fluor 555 goat anti-human IgG secondary antibody (1:200, Invitrogen). For AQP4 immunostaining cells were fixed in 4% paraformaldehyde (PFA) and permeabilized with 0.2% Triton-X. Rabbit anti-AQP4 antibody (1:200, Santa Cruz Biotech) was added followed by Alexa Fluor-488 goat anti-rabbit IgG secondary antibody (1:200, Invitrogen) for quantitative ratio image analysis, as described.²⁰

Complement- and cell-mediated cytotoxicity

For assay of CDC, cells were incubated for 60 min at 37 °C with NMO-IgG or NMO serum (control or EndoS-treated) with 2% human complement (Innovative Research, Novi, MI). In some experiments NMO-IgG was added 30 min before EndoS addition, followed 60 min later by complement. Cytotoxicity was measured by LDH release assay (Promega, Madison, WI) or live/dead cell staining, as described.²³ Calcein-AM and ethidium-homodimer (Invitrogen) were added to stain live cells green and dead cells red. For assay of ADCC, NK-92 cells expressing CD16 (Conkwest, San Diego, CA) were used as the effector cells. The AQP4-expressing CHO cells were incubated for 2 h at 37 °C with NMO-IgG and effector cells at an effector: target cell ratio of 20:1, followed by live-dead cell staining.

Ex vivo spinal cord slice model of NMO

Wild type and AQP4 null mice in a CD1 genetic background were used, as generated and characterized previously.⁵ Transverse slices of cervical spinal cord of thickness 300 μm were cut from 7-day old mice using a vibratome and placed in ice-cold Hank's balanced salt solution (HBSS, pH 7.2).²⁴ Slices were placed on transparent membrane inserts (Millipore, Millicell-CM 0.4 μm pores, 30 mm diameter) in 6-well plates containing 1 mL culture medium, with a thin film of culture medium covering the slices. Slices were cultured in 5% CO₂ at 37 °C for 7 days in 50% MEM, 25% HBSS, 25% horse serum, 1% penicillin-streptomycin, 0.65% glucose and 25 mM HEPES. On day 7, NMO-IgG (5 $\mu\text{g}/\text{mL}$ control or EndoS-treated) and human complement (5 %) were added to the culture medium on both sides of the slices. In some experiments NMO-IgG was first added, followed 30 min later by EndoS, and 60 min thereafter by complement. Slices were cultured for an additional 24 h, and immunostained for AQP4 and glial fibrillary acid protein (GFAP). Sections were scored as follows: 0, intact slice with normal GFAP and AQP4 staining; 1, mild astrocyte swelling and/or AQP4 staining; 2, at least one lesion with loss of GFAP and AQP4 staining; 3, multiple lesions affecting > 30 % of slice area; 4, lesions affecting > 80 % of slice area.

In vivo mouse brain injection models of NMO

Adult wild type mice (30–35 g) were anesthetized with 2,2,2-tribromoethanol (125 mg/kg i.p.) and mounted in a stereotactic frame. Following a midline scalp incision, a burr hole of

diameter 1 mm was made in the skull 2 mm to the right of bregma. A 30-gauge needle attached to 50- μ L gas-tight glass syringe (Hamilton) was inserted 3-mm deep to infuse 0.6 μ g NMO-IgG (control or EndoS-treated) and 3 μ L of human complement in a total volume of 8 μ L (at 2 μ L/min), as described.²⁵ In some experiments purified IgG from NMO serum (30 μ g) was injected together with an excess of EndoS-treated IgG purified from NMO or control serum (105 μ g) and 3 μ L human complement in a total volume of 18 μ L. After 3 days mice were anesthetized and perfused through the left cardiac ventricle with 5 mL PBS and then 20 mL of PBS containing 4% PFA. Brains were post-fixed for 2 hours in 4% PFA. Five μ m-thick paraffin sections were immunostained at room temperature for 1 h with: rabbit anti-AQP4 (1:200, Santa Cruz Biotechnology, Santa Cruz, CA), mouse anti-GFAP (1:100, Millipore, Temecula, CA), and goat anti-myelin basic protein (MBP) (1:200, Santa Cruz Biotechnology) followed by the appropriate fluorescent secondary antibody (1:200, Invitrogen). Tissue sections were examined with a Leica DM 4000 B microscope at 25x magnification. AQP4, GFAP and MBP immunonegative areas were defined by hand and quantified using ImageJ. Data are presented as percentage of immunonegative area (normalized to total area of hemi-brain slice). Mouse studies were approved by the UCSF Committee on Animal Research.

RESULTS

EndoS deglycosylation of NMO autoantibody prevents cytotoxicity

Fig. 1A diagrams N-linked glycosylation on asparagine-297 on the CH2 domain of both IgG heavy chains. EndoS selectively cleaves the β 1-4 linkage between two *N*-acetylglucosamines located in the conserved core of the N-linked glycan of IgG. Fig. 1B shows SDS-PAGE stained with Coomassie blue (top) and lectin blot (bottom) of control and EndoS-treated NMO-IgG or IgG from NMO patient sera. Lectin blot analysis using *Lens culinaris* agglutinin (LCA) recognizes α -linked mannose residues, showing loss of reactivity with removal of the glycan moiety. EndoS treatment resulted in IgG deglycosylation as seen by reduced molecular size by \sim 3 kDa of the heavy chains and loss of LCA signal. Deglycosylation was near complete by 60 min with 10 unit EndoS per 1 μ g IgG.

The major effector functions of NMO-IgG were abolished by EndoS treatment. Fig. 1C shows loss of CDC in AQP4-expressing cells by LDH release (top) and live/dead staining (bottom) assays. CDC was compared in cells exposed to control or EndoS-treated NMO-IgG, together with human complement. EndoS treatment prevented CDC in both AQP4-expressing CHO and U87MG cells, even at high antibody concentration. Fig. 1D shows loss of ADCC in AQP4-expressing cells by live/dead staining. ADCC was compared in cells exposed to control or EndoS-treated NMO-IgG together with human NK-cells.

Cytotoxicity measurements were also done using NMO sera, which contain a complex, polyclonal mixture of NMO antibodies. Fig. 2A (left) shows prevention of CDC by EndoS treatment in a NMO serum specimen, as revealed by LDH release (top) and live/dead staining (bottom). Data for three additional sera from different NMO patients are summarized in Fig. 2A (right). EndoS treatment (1 unit per μ g IgG for 60 min) greatly reduced CDC. Fig. 2C shows that EndoS treatment prevented ADCC in two NMO sera tested.

Having demonstrated that pre-treatment of NMO-IgG and NMO sera with EndoS prevents cytotoxicity, we tested whether post-treatment, after antibody binding to AQP4, is effective. For these studies AQP4-expressing cells were pre-incubated for 30 min with NMO-IgG, then EndoS was added, followed 30 min later by complement. Fig. 2C shows that post-

treatment with EndoS was effective, indicating EndoS deglycosylation of AQP4-bound NMO antibody can occur *in situ*.

EndoS deglycosylated NMO-IgG competes with binding of pathogenic NMO-IgG to AQP4

Quantitative measurements were done to determine whether EndoS treatment alters NMO-IgG binding to AQP4, which is expected to depend on the Fab rather than the Fc portion of the antibody. Binding was measured by two-color ratio imaging in which the NMO antibody was stained green (with Alexa-Fluor 555-conjugated anti-human secondary antibody) and AQP4 stained red (with anti-C-terminus rabbit primary antibody and Alexa Fluor-488-conjugated anti-rabbit secondary antibody). Fluorescence micrographs in Fig. 3A (left) show saturable antibody binding, with comparable red fluorescence for the control and EndoS-treated antibody. Fig. 3A (right) shows single-site binding curves for control and EndoS-treated NMO-IgG. Antibody binding was not significantly altered by EndoS. Similar measurements in Fig. 3B show that EndoS treatment did not affect AQP4 binding of IgG from serum of two NMO patients.

We reasoned that the EndoS deglycosylated antibody could function as a therapeutic antibody, in that it would be non-pathogenic and compete with pathogenic (untreated) NMO antibody for binding to AQP4. CDC was measured in AQP4-expressing cells treated with 2 or 5 $\mu\text{g/mL}$ NMO-IgG together with complement and different concentrations of EndoS-treated NMO-IgG. CDC was greatly reduced in a concentration-dependent manner when NMO-IgG was supplemented with excess EndoS-treated NMO-IgG (Fig. 3C). As a control, 40 $\mu\text{g/mL}$ EndoS-treated control (non-NMO) antibody did not protect against CDC produced by 2 or 5 $\mu\text{g/mL}$ NMO-IgG (not shown). Similarly, EndoS-deglycosylated NMO serum protected against CDC from untreated NMO serum (not shown). EndoS deglycosylation thus converts pathogenic NMO-IgG into a therapeutic blocking antibody.

EndoS treatment prevents lesions in an ex vivo spinal cord slice model of NMO

The efficacy of EndoS treatment was tested in a spinal cord slice culture model of NMO, in which NMO-IgG and complement produce lesions with loss of GFAP, AQP4 and myelin, deposition of activated complement, and activation of microglia.²⁴ Spinal cord slices were cultured for 7 d, after which NMO-IgG (control or EndoS-treated) and human complement were added to the culture medium on both sides of the slices. Following an additional 24 h in culture, slices were immunostained for GFAP and AQP4, and scored for lesion severity. Representative fluorescence micrographs in Fig. 4A and lesion scores in Fig. 4B show marked loss of GFAP and AQP4 in NMO-IgG and complement-treated spinal cord slices, but little loss of GFAP and AQP4 when NMO-IgG was replaced by NMO-IgG^{GL-}. To test the efficacy of EndoS treatment *in situ* after NMO-IgG binding to AQP4, NMO-IgG was first added to the slices, following by 20 U/mL EndoS 30 min later, and then by complement 60 min later. Representative fluorescence micrographs in Fig. 4C and lesion scores in Fig. 5D show that EndoS addition post-NMO-IgG prevented lesion development. EndoS alone did not cause damage to the slice cultures.

EndoS treatment prevents lesions in an in vivo mouse model of NMO

The efficacy of EndoS treatment was also tested in an *in vivo* mouse model of NMO produced by intracerebral injection of NMO-IgG and human complement.²⁵ Fig. 5A shows marked loss of AQP4, GFAP and myelin in brains of mice injected with NMO-IgG and human complement, in agreement with prior results.²⁵⁻²⁷ Fig. 5B shows a higher magnification of the lesion with loss of AQP4, GFAP and myelin compared to non-injected contralateral hemisphere. Lesions are surrounded by reactive astrocytes that overexpress the astrocyte marker GFAP (Fig. 5B). Replacement of NMO-IgG with the same concentration of NMO-IgG^{GL-} produced little loss of AQP4, GFAP and myelin (Fig. 5A). Quantification

of lesion size showed near absence of astrocyte and oligodendrocyte injury with the EndoS-treated NMO-IgG (Fig. 5C).

To show that EndoS-treated NMO antibody can compete with pathogenic antibody in mouse brain, purified IgG from NMO patient serum was injected with an excess of EndoS-treated purified IgG from the same NMO patient or a control (non-NMO) serum, together with human complement. Fig. 5D shows marked loss of AQP4, GFAP and myelin with injection of NMO-IgG and excess EndoS-treated control IgG, whereas coinjection of NMO-IgG with an excess of EndoS-treated NMO-IgG greatly reduced lesion size.

DISCUSSION

EndoS treatment abolished NMO-IgG effector functions, preventing complement- and cell-mediated cytotoxicity without affecting binding to AQP4. Pathogenic NMO autoantibodies are thus converted enzymatically into therapeutic blocking antibodies, as deglycosylated NMO-IgG competes with pathogenic NMO-IgG for binding to AQP4. EndoS neutralized NMO-IgG effector function in multiple NMO sera, preventing CDC and ADCC in cell cultures, and the development of NMO pathology in available spinal cord slice culture and mouse models of NMO based on NMO-IgG and complement-dependent cytotoxicity. Testing of EndoS in more clinically relevant animal models of NMO is needed, if and when they become available.

EndoS was effective as well in neutralizing AQP4-bound NMO-IgG *in situ*, as cytotoxicity and NMO pathology were prevented when EndoS was added after NMO-IgG was fully bound to cell surface AQP4. Competition of EndoS-treated, deglycosylated NMO-IgG with untreated, pathogenic NMO-IgG was also shown, which was anticipated from prior studies showing that unrelated monoclonal recombinant NMO antibodies compete for binding to AQP4 with polyclonal NMO-IgG in NMO patient sera.¹⁰ The large size of NMO-IgG compared to AQP4 is the molecular basis of this steric competition. Our findings suggest the potential utility of EndoS or alternative IgG-selective endoglycosidases for NMO therapy.

One potential approach for implementation of EndoS therapy in NMO would involve treatment of whole blood with EndoS by, for example, therapeutic apheresis involving passage of patient blood through an extracorporeal cartridge containing surface-immobilized EndoS. The EndoS-treated NMO-IgG would not cause pathology itself, and compete for binding to AQP4 with remaining or newly generated pathogenic NMO-IgG. Because the EndoS-treated NMO-IgG blocks binding of pathogenic NMO-IgG, incomplete IgG deglycosylation should be adequate. An alternative approach would involve *ex vivo* EndoS treatment of plasma obtained by plasmapheresis, followed by re-administration of the treated, autologous plasma. An immune response is unlikely following EndoS treatment of autologous blood or plasma. The EndoS-treated plasma or purified IgG could be introduced intravenously, or by intrathecal or retro-orbital routes to target NMO lesions with minimal systemic exposure.

Because of its high selectivity, EndoS administration *in vivo* has potential therapeutic value in NMO, though safety and immunogenicity are significant concerns. EndoS is the only known endoglycosidase that selectively hydrolyzes glycans on IgG, without affecting IgA, IgM or other glycoproteins.¹⁴ Other endoglycosidases, such as EndoF₁₋₃ from *Elizabethkingia meningoseptica*, or EndoE from *Enterococcus faecalis*, cleave glycans on many glycoproteins. Intravenous injection of 10 µg EndoS in mice prevented the development of lupus-like disease in a model of spontaneous lupus without observed toxicity.¹⁵ Repeated injections of EndoS in rabbits produced an anti-EndoS antibody response, but did not alter EndoS pharmacokinetics or endoglycosidase activity.¹⁵

Intravenous EndoS administration in humans is predicted to neutralize IgG globally, but likely cause an immune response, precluding chronic administration, but potentially allowing its use in acute disease exacerbations. Intrathecal or retro-orbital administration of EndoS would minimize these concerns, targeting EndoS to NMO lesions in spinal cord and optic nerve.

In conclusion, EndoS neutralization of pathogenic anti-AQP4 autoantibody adds to the list of potential new therapies for NMO. Notwithstanding issues about manufacturing, potential toxicity and immunogenicity, enzymatic neutralization provides a unique approach in that it transforms a patient's own polyclonal NMO-IgG into non-pathogenic, therapeutic antibodies that target the initiating pathogenic event in NMO.

Acknowledgments

This work was supported by grants from the Guthy-Jackson Charitable Foundation, and grants EY13574, EB00415, DK35124, HL73856, DK86125 and DK72517 from the National Institutes of Health.

Abbreviations

ADCC	antibody-dependent cell-mediated cytotoxicity
AQP4	aquaporin-4
CDC	complement-dependent cytotoxicity
EndoS	endoglycosidase S
NMO	neuromyelitis optica
NMO-IgG	neuromyelitis optica immunoglobulin G
NMO-IgG^{GL-}	EndoS-treated NMO-IgG
NMO serum^{GL-}	EndoS-treated NMO serum

References

- Jarius S, Paul F, Franciotta D, et al. Mechanisms of disease: aquaporin-4 antibodies in neuromyelitis optica. *Nat Clin Pract Neurol*. 2008; 4:202–214. [PubMed: 18334978]
- Wingerchuk DM, Lennon VA, Lucchinetti CF, et al. The spectrum of neuromyelitis optica. *Lancet Neurol*. 2007; 6:805–815. [PubMed: 17706564]
- Lennon VA, Kryzer TJ, Pittock SJ, et al. IgG marker of optic-spinal multiple sclerosis binds to the aquaporin-4 water channel. *J Exp Med*. 2005; 202:473–477. [PubMed: 16087714]
- Jarius S, Wildemann B. AQP4 antibodies in neuromyelitis optica: diagnostic and pathogenetic relevance. *Nat Rev Neurol*. 2010; 6:383–392. [PubMed: 20639914]
- Manley GT, Fujimura M, Ma T, et al. Aquaporin-4 deletion in mice reduces brain edema after acute water intoxication and ischemic stroke. *Nat Med*. 2000; 6:159–163. [PubMed: 10655103]
- Nielsen S, Nagelhus EA, Amiry-Moghaddam M, et al. Specialized membrane domains for water transport in glial cells: high-resolution immunogold cytochemistry of aquaporin-4 in rat brain. *J Neurosci*. 1997; 17:171–180. [PubMed: 8987746]
- Papadopoulos MC, Verkman AS. Aquaporin-4 and neuromyelitis optica. *Lancet Neurol*. 2012; 11:535–544. [PubMed: 22608667]
- Collongues N, de Seze J. Current and future treatment approaches for neuromyelitis optica. *Ther Adv Neurol Disord*. 2011; 4:111–121. [PubMed: 21694808]
- Cree B. Neuromyelitis optica: diagnosis, pathogenesis, and treatment. *Curr Neurol Neurosci Rep*. 2008; 8:427–433. [PubMed: 18713580]

10. Tradtrantip L, Zhang H, Saadoun S, et al. Anti-aquaporin-4 monoclonal antibody blocker therapy for neuromyelitis optica. *Ann Neurol.* 2012; 71:314–322. [PubMed: 22271321]
11. Tradtrantip L, Zhang H, Saadoun S, et al. Small-molecule inhibitors of NMO-IgG binding to aquaporin-4 reduce astrocyte cytotoxicity in neuromyelitis optica. *FASEB J.* 2012; 26:2197–2208. [PubMed: 22319008]
12. Jefferis R, Lund J, Pound JD. IgG-Fc mediated effector functions: Molecular definition of interaction sites for effectors ligands and the role of glycosylation. *Immunol Rev.* 1008; 163:59–76. [PubMed: 9700502]
13. Alhorn M, Olin A, Nimmerjahn F, et al. Human IgG/Fc γ R interactions are modulated by streptococcal IgG glycan hydrolysis. *PLoS ONE.* 2008; 3:e1413. [PubMed: 18183294]
14. Collin M, Olsen A. EndoS, a novel secreted protein from *Streptococcus pyogenes* with endoglycosidase activity on human IgG. *EMBO.* 2001; 20:3046–3055.
15. Nandakumar KS, Collin A, Olisen A, et al. Endoglycosidase treatment abrogates IgG arthritogenicity-importance of IgG glycosylation in arthritis. *Eur J Immunol.* 2007; 37:2973–2982. [PubMed: 17899548]
16. Albert H, Collin M, Dudziak D, et al. In vivo enzymatic modulation of IgG glycosylation inhibits autoimmune disease in a IgG subclass-dependent manner. *Proc Natl Acad Sci USA.* 2008; 105:15005–15009. [PubMed: 18815375]
17. van Timmeren MM, van der Veen BS, Stegeman CA, et al. IgG glycan hydrolysis attenuates ANCA-mediated glomerulonephritis. *J Am Soc Nephrol.* 2010; 21:1103–1114. [PubMed: 20448018]
18. Olsson ML, Clausen H. Modifying the red cell surface: towards an ABO-universal blood supply. *Br J Haematol.* 2008; 140:3–12. [PubMed: 17970801]
19. Liu QP, Sulzenbacher G, Yuan H, et al. Bacterial glycosidases for the production of universal red blood cells. *Nat Biotechnol.* 2007; 25:454–464. [PubMed: 17401360]
20. Crane JM, Lam C, Rossi A, et al. Binding affinity and specificity of neuromyelitis optica autoantibodies to aquaporin-4 M1/M23 isoforms and orthogonal arrays. *J Biol Chem.* 2011; 286:16516–16524. [PubMed: 21454592]
21. Bennett JL, Lam C, Kalluri SR, et al. Intrathecal pathogenic anti-aquaporin-4 antibodies in early neuromyelitis optica. *Ann Neurol.* 2009; 66:617–629. [PubMed: 19938104]
22. Wingerchuk DM, Lennon VA, Pittock SJ, et al. Revised diagnostic criteria for neuromyelitis optica. *Neurology.* 2006; 66:1485–1489. [PubMed: 16717206]
23. Phaun PW, Ratelade J, Rossi A, et al. Complement-dependent cytotoxicity in neuromyelitis optica requires aquaporin-4 assembly in orthogonal arrays. *J Biol Chem.* 2012; 287:13829–13839. [PubMed: 22393049]
24. Zhang H, Bennett JL, Verkman AS. Ex vivo spinal cord slice model of neuromyelitis optica reveals novel immunopathogenic mechanisms. *Ann Neurol.* 2011; 70:942–954.
25. Saadoun S, Waters P, Bell BA, et al. Intra-cerebral injection of neuromyelitis optica immunoglobulin G and human complement produces neuromyelitis optica lesions in mice. *Brain.* 2010; 133:349–361. [PubMed: 20047900]
26. Saadoun S, Waters P, Macdonald C, et al. Neutrophil protease inhibition reduces neuromyelitis optica immunoglobulin G-induced damage in mouse brain. *Ann Neurol.* 2012; 71:323–333. [PubMed: 22374891]
27. Ratelade J, Zhang H, Saadoun S, et al. Neuromyelitis optica IgG and natural killer cells produce NMO lesions in mice without myelin loss. *Acta Neuropath.* 2012; 123:861–872. [PubMed: 22526022]

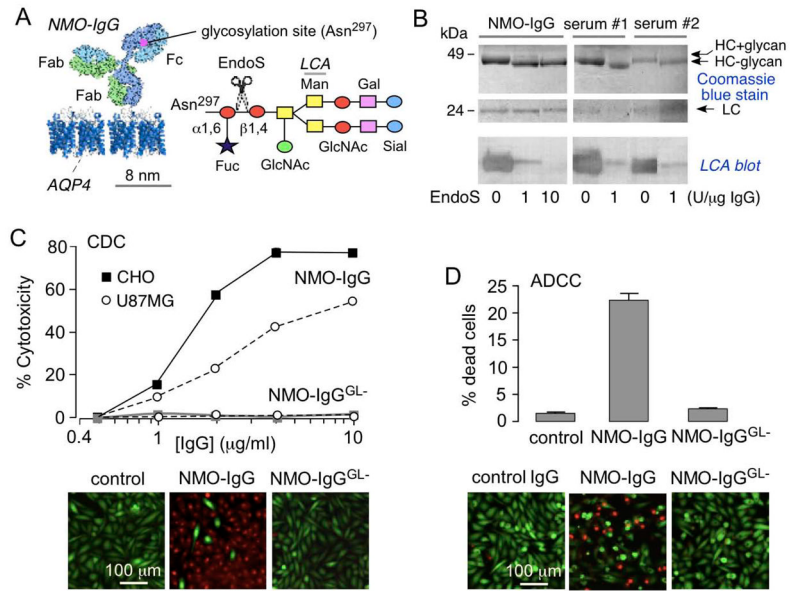


Figure 1. EndoS deglycosylation of NMO-IgG prevents CDC and ADCC
A. (left) Schematic of IgG showing the Fc glycosylation at Asn-297, and Fab binding to AQP4. (right) Sugar moiety at Asn-297 with EndoS cleavage site shown. Asn, asparagine; Fuc, fucose; GlcNAc, N-acetylglucosamine; Man, mannose; Gal, galactose; Sial, sialic acid.
B. Coomassie blue SDS-PAGE and *Lens culinaris* agglutinin (LCA) lectin blot of control and EndoS-treated NMO-IgG and purified IgG from NMO sera. **C.** (top) CDC in AQP4-expressing CHO and U87MG cells incubated with NMO-IgG or NMO-IgG^{GL-} and 2% human complement, as quantified by LDH release (S.E., n=4). (bottom) Live/dead (green/red) staining of AQP4-expressing CHO cells incubated with 5 μg/mL NMO-IgG or NMO-IgG^{GL-} and 2% human complement. **D.** ADCC in AQP4-expressing CHO cells incubated with NK-cells and 20 μg/mL NMO-IgG or NMO-IgG^{GL-}, as quantified by percentage dead cells (S.E., n=4). (bottom) Live/dead (green/red) staining.

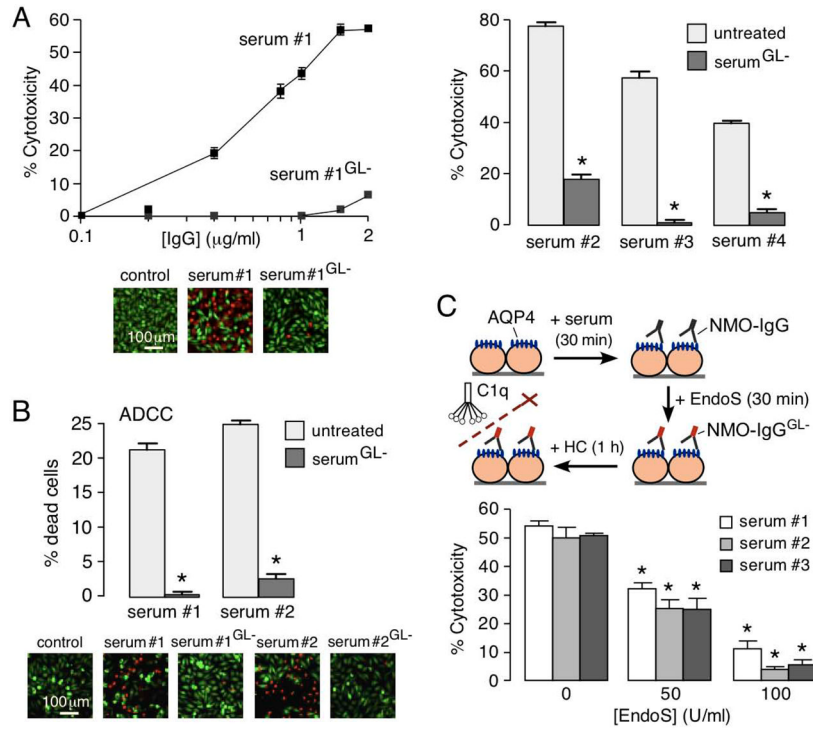


Figure 2. EndoS deglycosylation of NMO serum prevents CDC and ADCC

A. (left) CDC in AQP4-expressing CHO cells incubated with NMO serum or NMO serum^{GL-} and 2% human complement, as quantified by LDH release (top) and live/dead staining (bottom). (right) Summary of data from three NMO sera (S.E., n=6, P < 0.001). **B.** ADCC in AQP4-expressing CHO cells incubated with NK-cells and control or EndoS-treated IgG from NMO sera (1 mg/mL), as quantified by percentage dead cells (S.E., n=5, P < 0.001). (bottom) Live/dead (green/red) staining. **C.** EndoS addition *in situ* after NMO-IgG binding to AQP4 reduces CDC. CDC was measured by LDH release in AQP4-expressing CHO cells incubated with NMO serum for 30 min, then treated with EndoS for 30 min, followed by 2% human complement for 1 h. (S.E., n=4, * P < 0.01).

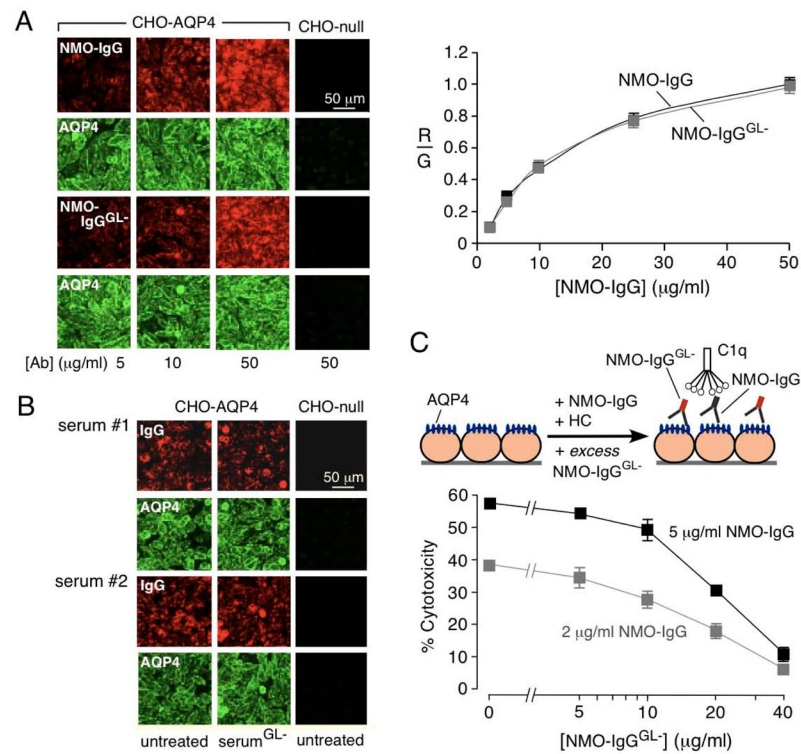


Figure 3. EndoS-treated NMO-IgG binds to AQP4 and competes with binding of pathogenic NMO-IgG

A. Binding of NMO-IgG to AQP4 in CHO cells. (left) Fluorescence micrographs of AQP4-expressing CHO cells stained for NMO-IgG or NMO-IgG^{GL-} (red) and AQP4 (green). (right) Binding of NMO-IgG and NMO-IgG^{GL-} showing red-to-green fluorescence ratio (R/G) as a function of NMO-IgG concentration (S.E., n=3). Differences not significant. **B.** Binding of control and EndoS-treated NMO patient serum to AQP4 on CHO cells. **C.** EndoS-treated NMO-IgG protects against CDC caused by (untreated) NMO-IgG. LDH release assayed in CHO cells after 1 h incubation with indicated concentrations of NMO-IgG and NMO-IgG^{GL-}, together with 2% human complement.

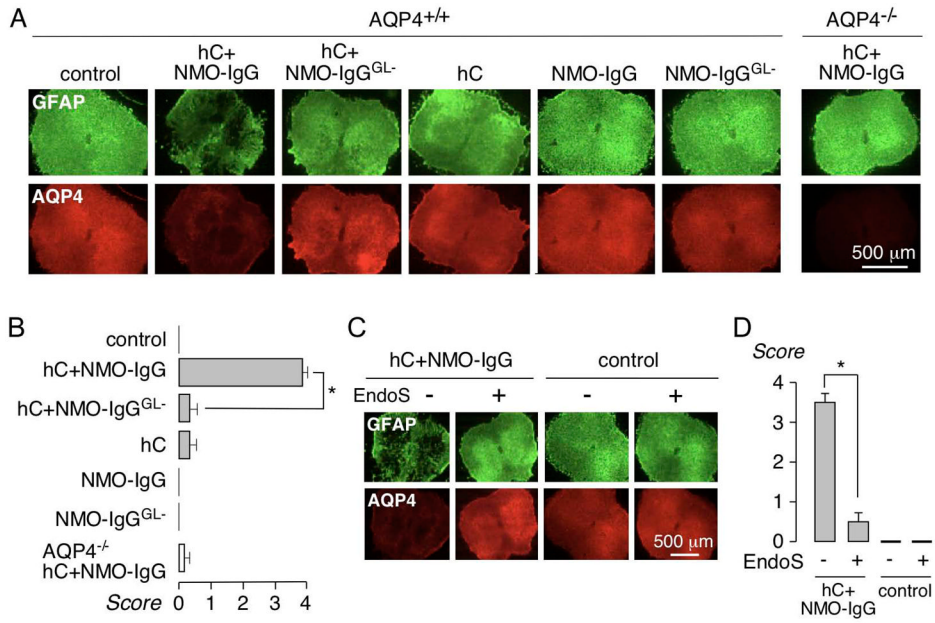


Figure 4. EndoS treatment prevents lesions in an *ex vivo* spinal cord slice culture model of NMO
A. Spinal cord slice cultures were exposed to 5 $\mu\text{g}/\text{mL}$ NMO-IgG or NMO-IgG^{GL-} and 5% human complement (HC). Representative GFAP and AQP4 immunofluorescence shown after 24 h. **B.** Summary of lesion scores from experiments as in A (S.E., 6 slices per group, * $P < 0.01$). **C.** Slice cultures were incubated with 5 $\mu\text{g}/\text{mL}$ NMO-IgG, and then 30 min later with 20 U/mL EndoS, and 5 % HC added 60 min later. **D.** Lesion scores (S.E., 6 slices per group, * $P < 0.01$).

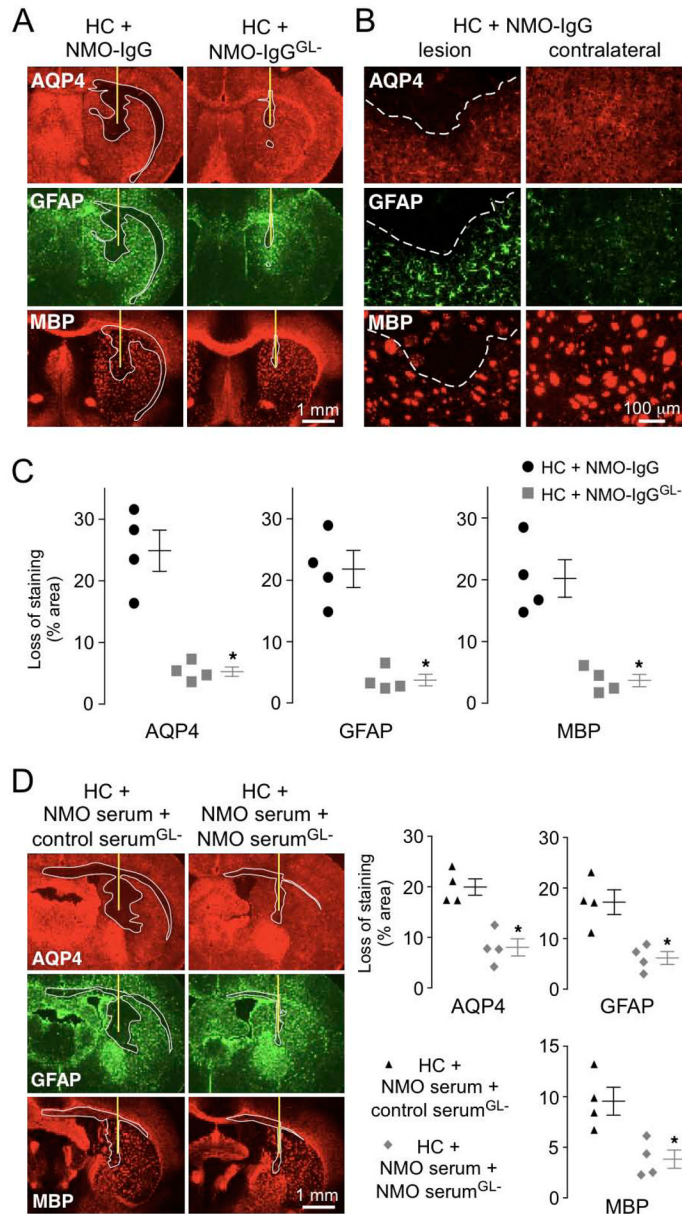


Figure 5. EndoS treatment prevents lesions in an *in vivo* mouse model of NMO

A. Brains of live mice were injected with 0.6 μ g NMO-IgG or NMO-IgG^{GL-} together with 3 μ L human complement (HC). Representative GFAP, AQP4 and myelin (MBP) immunofluorescence at 3 days after injection. Yellow line represents needle tract. White line delimits the lesion with loss of AQP4, GFAP and myelin. **B.** Higher magnification of brains injected with NMO-IgG and HC. White dashed line delimits the lesion (top). Contralateral hemispheres (non-injected) are shown (right). **C.** Summary of lesion size from experiments as in A (S.E., 4 mice per group, * $P < 0.01$ by the non parametric Mann-Whitney test). **D.** Brains were injected with 30 μ g of purified IgG from NMO serum and 105 μ g of EndoS-treated IgG purified from the same NMO patient (NMO serum^{GL-}) or a non-NMO control (control serum^{GL-}), together with 3 μ L HC. (left) Representative GFAP, AQP4 and MBP immunofluorescence at 3 days after injection. Yellow line shows the needle tract and white

line delimits the lesion. (right) Summary lesion size (S.E., 4 mice per group, * $P < 0.01$ by the non parametric Mann-Whitney test).